Homoleptic Cerium tris(Dialkylamido)imidophosphorane Guanidinate Complexes

SCHOLARONE™
Manuscripts

ARTICLE

Homoleptic Cerium *tris*(Dialkylamido)imidophosphorane Guanidinate Complexes

Luis M. Aguirre Quintana,[a] Ningxin Jiang,[a] John Bacsa,[a] and Henry S. La Pierre*[ab]

We report the synthesis of a new potassium tris(piperdino)imidophosphorane N,N'-dicyclohexylguanidinate, K[^{Cy}GNP(pip)$_3$], and describe the synthesis and characterization of the tris-homoleptic compounds, [Ce(^{Cy}GNP(pip)$_3$)$_3$], **1-Ce**, and [Ce(^{Cy}GNP(pip)$_3$)$_3$][BPh$_4$], **2-Ce**. The latter is an unusual cationic tetravalent cerium complex. Cyclic voltammetry studies of **1-Ce** and **2-Ce** revealed E$_{pc}$ potentials of -1.56 V and -1.81 V, and E$_{pa}$ potentials of -0.78 V and -0.66 V (200 mV/s; THF, vs. Fc0/+), respectively. Compounds **1-Ce** and **2-Ce** were studied by L$_3$-edge X-ray absorption near-edge spectroscopy (XANES), and the spectrum of **2-Ce** revealed a white-line multiplet with an nf value of 0.50(2).

Introduction

Synthetic methods to isolate tetravalent lanthanide ions are vital tools to enable the application of these high-valent ions in components of quantum information technologies.[1-4] Additionally, detailed understanding of ligand effects on the redox properties of the trivalent lanthanides may facilitate the development of novel intralanthanide separations.[5-7] In practice, it is difficult to produce molecular tetravalent lanthanide compounds other than those of cerium. However, the redox properties of molecular cerium complexes are exceptionally sensitive to their coordination environment.[8-10] Therefore coordination and redox studies of cerium[1, 11, 12] serve as a guidepost for the isolation and characterization of tetravalent terbium[7, 13, 14] and praseodymium[15] complexes as has recently been demonstrated. These examples of unusual molecular tetravalent lanthanide complexes are supported by either *tris*(dialkylamido)imidophosphorane, ([NP(NR$_2$)$_3$]$^-$), or *tris*(alkoxy)siloxide/*tris*(phenyl)siloxide ligands. These ligands are both principally monodentate 1σ, 2π weak-field donors that also provide steric protection to the metal center.[13, 16] In order to examine the synergy between the number of ligand donor atoms and the stabilization of high-valent lanthanides, guanidinate ligands supported by the *tris*(dialkylamido)imidophosphorane, ([NP(NR$_2$)$_3$]$^-$), were prepared.

Guanidinates are bulky weak-field ligands[17-19], but differ from imidophosphoranes and siloxides in that they operate as bidentate ligands.[19, 20] Most guanidinate ligands possess a dialkylamido moiety in their backbone that makes them more basic donors than their amidinate or formamidinate counterparts.[18, 21-24] There have been iterations of guanidinates with different backbones such as ketimides[25] and imidazoline-2-iminates,[26] however there are no examples of the guanidinates with a [NP(NR$_2$)$_3$]$^-$ supporting moiety. Tris(dialkylamido)imidophosphoranes have a zwitterionic ylide-like (i.e. [(N^{2-}–P$^+$(NR$_2$)$_3$])[16] resonance structure that poises them to act as uniquely basic donors in a guanidinate ligand framework. As a result, they are attractive candidates to stabilize tetravalent lanthanide compounds. Herein we present the synthesis of a new tris(piperdino)imidophosphorane N,N'-dicyclohexylguanidinate ligand, and the isolation of its *tris*-homoleptic Ce^{3+} and Ce^{4+} complexes. These metal complexes were studied by cyclic voltammetry and L$_3$-edge X-ray

Scheme 1: Synthesis of **1-K**, **1-Ce**, and **2-Ce**.

a. Department of Chemistry and Biochemistry, Georgia Institute of Technology, Atlanta, Georgia 30332-0400, USA. E-mail: hsl@gatech.edu

b. Nuclear and Radiological Engineering Program, Georgia Institute of Technology, Atlanta, Georgia 30332-0400, USA.

2-Ce
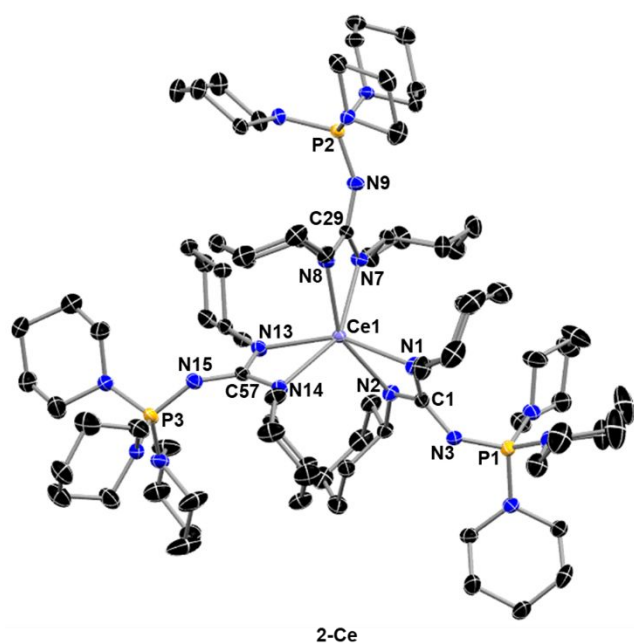
Figure 1. Molecular structure of **2-Ce** shown with thermal ellipsoids at 50% probability. Hydrogen atoms and the tetraphenylborate counteranion are omitted for clarity.

absorption near edge spectroscopy (XANES) in order to determine the relative stabilization of the tetravalent oxidation state in a homoleptic guanidinate coordination environment and the resultant changes and ground state multiconfigurational behaviour.

Results and discussion

Synthetic procedures

The synthesis of these metal complexes preceded via the isolation of the *tris*(piperdino)imidophosphorane N,N'-dicyclohexylguanidinate ligand precursor, $[K(THF)_2{}^{Cy}GNP(pip)_3]_2$ (**1-K**, Scheme 1). The reaction of the previously reported[11] $K[NP(pip)_3]$ with N,N'-dicyclohexylcarbodiimide in THF for 24 hours produced **1-K** in good yield, 89 %. The reaction of three equivalents of **1-K** with $CeCl_3(THF)_4$ yielded the greenish-yellow, *tris*-homoleptic Ce^{3+} complex, $[Ce(^{Cy}GNP(pip)_3)_3]$ (**1-Ce**) in 84 % yield. The *tris*-homoleptic, Ce^{4+} complex, $[Ce(^{Cy}GNP(pip)_3)_3]BPh_4$, **2-Ce** is then isolated from the reaction of **1-Ce** with $AgBPh_4$ in Et_2O in 81 % yield (Scheme 1).

X-ray crystallography

The molecular structure of **2-Ce**, as determined by single-crystal X-ray diffraction (SC-XRD), is shown in Figure 1. The structure of **1-Ce** is very similar (Figure S25). Compounds **1-Ce** and **2-Ce** both crystallize in the $P\bar{1}$ space group. The XRD analysis revealed the molecular structure of **1-Ce** to be a *tris*-homoleptic Ce^{3+} complex with three ligands coordinated to the cerium ion via a κ^2-guanidinate. The structure of **2-Ce** is charge-separated and is comprised of a $[Ce(^{Cy}GNP(pip)_3)_3]^{1+}$ cation that is structurally similar to **1-Ce**, and an outer-sphere $[BPh_4]^{1-}$ counteranion. In both structures, the 6-coordinate cerium complex adopted a propeller-like structure. Compound **2-Ce** is

one of a few crystallographically characterized cationic Ce^{4+} complexes reported to date.[27-30]

The average $Ce-N_{guan.}$ distance in **1-Ce** is 2.497(13) Å, and is similar to that observed in other trivalent cerium complexes.[31] Upon oxidation to **2-Ce** the average $Ce-N_{guan.}$ distance shortens to 2.355(13) Å. The contraction of the Ce–N on oxidation (0.142(13) Å) is in line with the expected difference in the Shannon ionic radii of 0.14 Å.[32] There is no change in the average $P-N_{imido}$ distance on oxidation (in **1-Ce** is 1.538(7) Å and in **2-Ce** is 1.548(2) Å, see Table 1). However, the average $P-N_{imido}-C_{guan.}$ angles in **1-Ce** and **2-Ce** are 133.76(17)° and 141.64(17)°, respectively. These metrics in **1-Ce** and **2-Ce** suggest that the imidophosphorane moiety of the ligand displays zwitterionic character (*i.e.* $[(N^{2-}-P^+(NR_2)_3])$ which may be accentuated upon oxidation (as indicated by the change in angle). The average $C_{guan.}-N_{guan.}$ and $C_{guan.}-N_{imido}$ distances in **1-Ce** are 1.343(3) Å and 1.390(3) Å respectively, suggesting partial double-bond character between the guanidinate carbon and the imidophosphorane nitrogen. Notably, the average $C_{guan.}-N_{guan.}$ and $C-N_{imido}$ distances in **2-Ce** are 1.355(3) Å and 1.348(3) Å respectively. From a purely structural standpoint, the changes in metal-ligand and intra-ligand bond-metrics upon oxidation of **1-Ce** to **2-Ce** suggest that the imidophosphorane backbone of the ligand participates in compensating for the change in the central metal's charge.

Table 1: Selected bond lengths and angles of **1-K**, **1-Ce**, and **2-Ce** as determined by single crystal X-ray diffraction.

Compound/Metric	1-K	1-Ce	2-Ce
Avg. $Ce-N_{guan.}$ dist.	N/A	2.497(13) Å	2.355(13) Å
Avg. $P-N_{imido}$ dist.	1.550(7) Å	1.538(7) Å	1.548(2) Å
Avg. $C_{guan.}-N_{imido}$ dist.	1.411(13) Å	1.390(3) Å	1.348(3) Å
Avg. $C_{guan.}-N_{guan.}$ dist.	1.341(10) Å	1.343(3) Å	1.355(3) Å
Avg. $N_{guan.}-C_{guan.}-N_{guan.}$ angle	116.0(9)°	113.61(12)°	110.53(19)°
Avg. $P-N_{imido}-C_{guan.}$ angle	127.8(7)°	133.76(17)°	141.64(17)°

Cyclic Voltammetry

Cyclic voltammetry (CV) measurements were performed on **1-Ce** and **2-Ce** and their cyclic voltammograms are shown in Figure 2. The cyclic voltammogram of **1-Ce**, performed at a scan rate of ν = 100 mV/s, shows an oxidation event at E_{pa} = -0.85 V (vs. $Fc^{0/+}$) and a return reduction at E_{pc} = -1.52 V (vs. $Fc^{0/+}$). Performing the measurement at higher scan rates showed a linear scan-rate dependence on the E_{pa} and E_{pc} as well as their corresponding i_{pa} and i_{pc} (see Figures S20 and S22) that resulted in redox events at E_{pa} = -0.62 V (vs. $Fc^{0/+}$) and E_{pc} = -1.69 V (vs. $Fc^{0/+}$) at a scan rate of ν = 800 mV/s. The cyclic voltammogram of **2-Ce**, performed under the same conditions as **1-Ce**, at a scan rate of ν = 100 mV/s showed a reduction at E_{pc} = -1.78 V (vs. $Fc^{0/+}$) and a returning oxidation at E_{pa} = -0.76 V (vs. $Fc^{0/+}$), while at a scan rate of ν = 800 mV/s E_{pc} = -1.97 V (vs. $Fc^{0/+}$) and E_{pa} = -
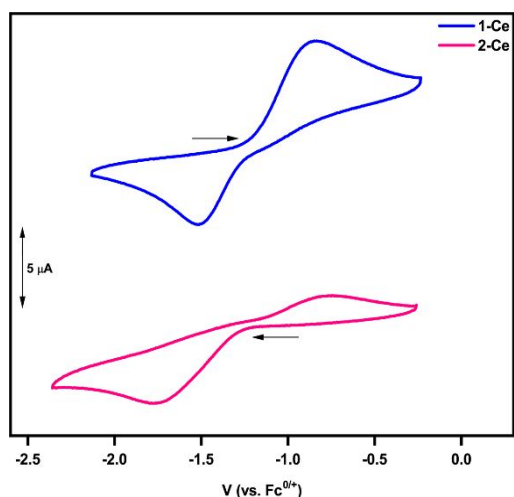
**Figure 2:** Cyclic voltammograms of **1-Ce,** and **2-Ce**, at 3.0 mM analyte and 0.1 M [(^{n}Bu)$_4$N][PF$_6$] at 100 mV/s . All potentials are referenced versus Fc$^{0/+}$ in THF.


Figure 3. Co-plot of UV-vis-NIR absorption spectra of **1-Ce** (blue, 1.2 mM, THF) and **2-Ce** (magenta, 2.45 μM, THF). The ^ symbol denotes the grating change and * denotes an instrumental artefact.

0.46 V (vs. Fc$^{0/+}$). The linear relationship between peak current and ν^{-2} observed in the Randles-Sevcik plots for **1-Ce** and **2-Ce**. (See Figures S21 and S23) suggest that the Ce$^{3+/4+}$ and Ce$^{4+/3+}$ redox events are both diffusion-controlled.[33]

To properly situate these electrochemical measurements in the broader context of cerium electrochemistry, the measured E$_{pc}$ of **1-Ce** and **2-Ce** are ~1 V less reducing than the E$_{pc}$ reported for [KCe(NP(1,2-*bis*-^{t}Bu-diamidoethane)(NEt$_2$))$_4$] and [KCe(NP(pip)$_3$)$_4$].[9] Only a few other examples of cerium compounds have more negative E$_{pc}$ potentials than **2-Ce**. These systems include [Li$_2$Ce(N=C^{t}BuPh)$_6$],[34] [Ce(L')(O^{t}Bu)$_2$][35] (where L' = 1,1'-di(2,4-bis-tert-butyl-salicylimino)ferrocenyl)), [Ce(L'')(O^{t}Bu)$_2$][35] (where L'' = 1,1'-di(2-tert-butyl-salicyl-(bis-phenyl)-iminophosphorano)ferrocenyl), and [Ce(2-(^{t}BuNO)Py)$_4$][36]. These examples present an E$_{pc}$ ~400 mV more negative than **2-Ce**. However, these examples are of neutral and anionic compounds. When compared to some of the previously described *cationic* Ce^{4+} compounds, more specifically those bearing TriNOx[28] and Atrane[30] ligands, **2-Ce** has an E$_{pc}$ ~500-600 mV more negative. The experimentally measured E$_{pc}$ of the previously reported tris-homoleptic guanidinate [Ce((^{i}PrN)$_2$CN(SiMe$_3$)$_2$)$_3$] (-0.56 V, vs. Fc$^{0/+}$)[37] is remarkably ~1 V more positive than the E$_{pc}$ of **1-Ce** and **2-Ce**. This example best highlights the direct impact of the imidophosphorane backbone of this guanidinate ligand on the Ce$^{3+/4+}$ couple.

UV-Visible-Near-Infrared spectroscopy

UV-visible-Near-Infrared (UV-Vis-NIR) spectra were acquired for **1-Ce** and **2-Ce** as solutions in THF (Figure 3). The UV-Vis-NIR spectrum of **1-Ce** displayed two absorption features at 376 nm (ε = 368 cm^{-1}M^{-1}) and 452 nm (ε = 543 cm^{-1}M^{-1}). The molar absorptivity coefficients of these absorption features are well within the range for the expected ^{2}F → ^{2}D transitions characteristic of a Ce^{3+} ion.[38, 39] The UV-Vis-NIR spectrum of **2-Ce** exhibits a broad and intense transition centered at 575 nm (ε = 4017 cm^{-1}M^{-1}), and a less broad but intense transition at 355 nm (ε = 4765 cm^{-1}M^{-1}), both representative of ligand-to-metal charge transfer bands, which can be frequently observed in Ce^{4+}
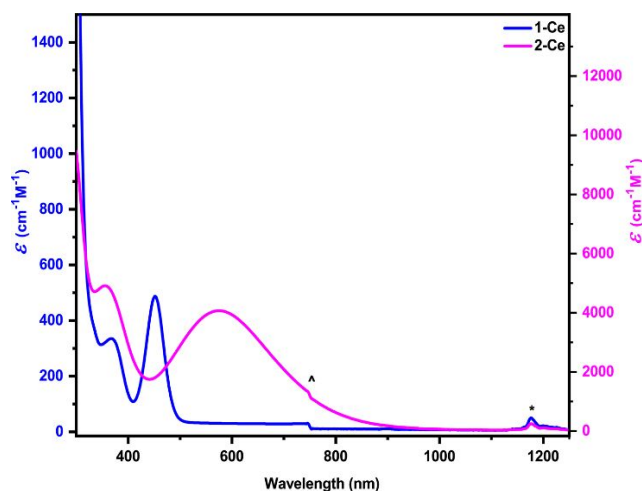
4f^0 complexes.[40] The normalized excitation and emission spectra of **1-Ce** (See Figure S18) presents excitation bands at 315 nm, 375 nm, 442 nm, and 464 nm and a broad emission band at 525 nm. In contrast to other Ce^{3+} tris-homoleptic guanidinate compounds,[31] the relative intensities of the excitation bands of **1-Ce** are nearly equivalent and the difference in the energies of the maxima is decreased. Another contrast to literature Ce^{3+} homoleptic guanidinate complexes with dialkylamide backbones is that the emission band of **1-Ce** does not exhibit a resolvable shoulder feature corresponding to the ^{2}D → ^{2}F$_{7/2}$ transition.[31]

Ce L$_3$-edge X-ray absorption near edge spectroscopy (XANES)

Ce L$_3$-edge XANES was used to investigate the impact of the [^{Cy}GNP(pip)$_3$]$^-$ ligand on the ground-state electronic structure of **1-Ce** and **2-Ce**. As described in our previous work,[11] the cerium L$_3$-edge is the electric-dipole allowed transitions arising from the cerium 2p orbital electrons excited to the unoccupied 5d states, 2p^{6}4f^{n}5d^0 → 2p^{5}4f^{n}5d^1. To guide our discussion and analysis of the Ce L$_3$-edge spectra of **1-Ce** and **2-Ce**, both spectra were fit using pseudo-Voigt functions and a single step function.

The Ce L$_3$-edge XANES spectrum of **1-Ce** (Figure S23) shows a single white-line feature and is characteristic of a Ce^{3+} ion.[41] In contrast, spectrum of **2-Ce** displayed a white-line doublet, diagnostic of Ce^{4+} compounds.[1, 9, 11, 41, 42] This feature is considered to be the result of a multiconfigurational ground state that consists of partial 2p^{6}4f^{n}5d^{0}L and 2p^{6}4f^{n+1}5d^{0}L̲ (where L̲ is a ligand hole) character that transition to the excited states 2p^{5}4f^{n}5d^{1}L and 2p^{5}4f^{n+1}5d^{1}L̲, respectively.[41-45] The ratio between the intensity of the first feature to the sum of the intensity of both features that comprise the white-line doublet is referred to as n_f and is a measure of the multiconfigurational nature of the ground state wavefunction. The spectrum of **2-Ce** was fit using four pseudo-Voigt functions [p2 [purple trace), p3 (orange trace), p4 (pink trace), and p5 (green trace)], and another Voigt function (p1) was included to fit the observed pre-edge feature that arises from a quadrupole-allowed 2p$_{3/2}$ →

ARTICLE
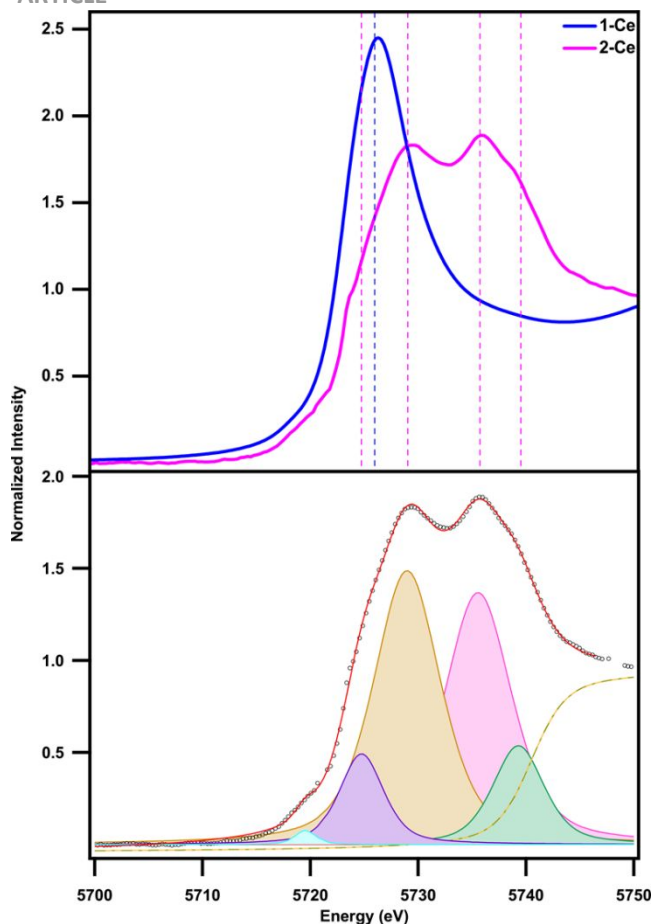
Figure 4. Top: Co-plotted experimental data of Ce L$_3$-Edge XAS absorption spectra for **1-Ce** (blue) and **2-Ce** (magenta). Bottom: Ce L$_3$-edge XAS experimental data (black) obtained for **2–Ce** and the pseudo-Voigt [purple (p2), orange (p3), pink (p4), and green (p5)] and step-like functions (yellow and gray dashed line), which sum to generate the curve fit (red).

4f transition [p1 (blue trace)], as shown in Figure 4. The energies of the white-line doublet maxima are 5729.0(7) eV and 5735.6(10) eV for **2-Ce**. The n_f value corresponding to the two white-line features for **2-Ce** is 0.50(2): where n_f = (Ap$_2$ + Ap$_3$)/(Ap$_2$ + Ap$_3$ + Ap$_4$ + Ap$_5$). The n_f value of **2-Ce** is higher than that of [Ce(NP(pip)$_3$)$_4$] (n_f = 0.38(2))[9] and [Ce(NP*)$_4$] (n_f = 0.40(4)),[9] and smaller than that of cerocene (n_f = 0.82(3))[44, 46], and is statistically equivalent to that observed for ceria (n$_f$ = 0.56(4))[47] and [CeCl$_6$]$^{2-}$ (n_f = 0.51(5)).[41] This observation is notable since **2-Ce** is a cationic Ce^{4+} complex, while the other two materials are either neutral or anionic.

Conclusions

In summary, we have reported the synthesis of a homoleptic Ce^{3+} complex, **1-Ce**, supported by the new *tris*(dialkylamido)imidophosphorane guanidinate ligand, [^{Cy}GNP(pip)$_3$]$^-$ that was subsequently oxidized with AgBPh$_4$ to yield the cationic homoleptic Ce^{4+} complex, **2-Ce**. The bond metrics of both **1-Ce** and **2-Ce** display noticeable differences between the Ce^{3+} and Ce^{4+} complexes while maintained under a similar coordination environment, thus allowing for an analysis of how this new ligand framework accommodates the oxidized metal center. Cyclic voltammetry demonstrates, in the

case of **2-Ce**, a remarkably negative E$_{pc}$. The cerium L$_3$-edge XANES data for both **1-Ce** and **2-Ce** revealed from a spectroscopic standpoint how the donor profile of this ligand framework stabilizes the tetravalent oxidation state of cerium, with similar multiconfigurational behaviour to that observed in anionic and neutral Ce^{4+} materials for the cationic, tetravalent cerium complex, **2-Ce**. These results poise this new ligand and its derivatives as an attractive system to build high-valent chemistry of lanthanides.

Conflicts of interest

There are no conflicts to declare.

Acknowledgements

1.   T. P. Gompa, A. Ramanathan, N. T. Rice and H. S. La Pierre, The Chemical and Physical Properties of Tetravalent Lanthanides: Pr, Nd, Tb, and Dy, *Dalton Trans.*, 2020, DOI: 10.1039/D0DT01400A.
2.   A. Gaita-Ariño, F. Luis, S. Hill and E. Coronado, Molecular spins for quantum computation, *Nat. Chem.*, 2019, **11**, 301-309.
3.   R. J. Blagg, L. Ungur, F. Tuna, J. Speak, P. Comar, D. Collison, W. Wernsdorfer, E. J. L. McInnes, L. F. Chibotaru and R. E. P. Winpenny, Magnetic relaxation pathways in lanthanide single-molecule magnets, *Nat. Chem.*, 2013, **5**, 673-678.
4.   G. Cao, Y. Qian, Z. Chen and Y. Zhang, Pr-O chemical bonding effect and Pr valence state in PrBa$_2$Cu$_3$O$_7$: A comprehensive structural-correlation study, *J. Phys. Chem. Solids*, 1995, **56**, 981-988.
5.   H. B. Lee, J. A. Bogart, P. J. Carroll and E. J. Schelter, Structural and electrochemical characterization of a cerium(IV) hydroxamate complex: implications for the beneficiation of light rare earth ores, *Chem. Commun.*, 2014, **50**, 5361-5363.
6.   J. J. M. Nelson and E. J. Schelter, Sustainable Inorganic Chemistry: Metal Separations for Recycling, *Inorg. Chem.*, 2019, **58**, 979-990.
7.   A. R. Willauer, C. T. Palumbo, R. Scopelliti, I. Zivkovic, I. Douair, L. Maron and M. Mazzanti, Stabilization of the Oxidation State +IV in Siloxide-Supported Terbium Compounds, *Angew. Chem. Int. Ed.*, 2020, **59**, 3549-3553.
8.   N. A. Piro, J. R. Robinson, P. J. Walsh and E. J. Schelter, The Electrochemical Behavior of Cerium(III/IV) Complexes: Thermodynamics, Kinetics and Applications in Synthesis, *Coord. Chem. Rev.*, 2014, **260**, 21-36.
9.   N. T. Rice, I. A. Popov, D. R. Russo, T. P. Gompa, A. Ramanathan, J. Bacsa, E. R. Batista, P. Yang and H. S. La Pierre, Comparison of Tetravalent Cerium and Terbium ions in a conserved, Homoleptic Imidophosphorane Ligand Field, *Chem. Sci.*, 2020, **11**, 6149-6159.
10.   R. Anwander, M. Dolg and F. T. Edelmann, The Difficult Search for Organocerium(IV) Compounds, *Chem. Soc. Rev.*, 2017, **46**, 6697-6709.

11. N. T. Rice, J. Su, T. P. Gompa, D. R. Russo, J. Telser, L. Palatinus, J. Bacsa, P. Yang, E. R. Batista and H. S. La Pierre, Homoleptic Imidophosphorane Stabilization of Tetravalent Cerium, *Inorg. Chem.*, 2019, **58**, 5289-5304.

12. R. P. Kelly, L. Maron, R. Scopelliti and M. Mazzanti, Reduction of a Cerium(III) Siloxide Complex To Afford a Quadruple-Decker Arene-Bridged Cerium(II) Sandwich, *Angew. Chem. Int. Ed.*, 2017, **56**, 15663-15666.

13. N. T. Rice, I. A. Popov, D. R. Russo, J. Bacsa, E. R. Batista, P. Yang, J. Telser and H. S. La Pierre, Design, Isolation, and Spectroscopic Analysis of a Tetravalent Terbium Complex, *J. Am. Chem. Soc.*, 2019, **141**, 13222-13233.

14. C. T. Palumbo, I. Zivkovic, R. Scopelliti and M. Mazzanti, Molecular Complex of Tb in the +4 Oxidation State, *J. Am. Chem. Soc.*, 2019, **141**, 9827-9831.

15. A. R. Willauer, C. T. Palumbo, F. Fadaei-Tirani, I. Zivkovic, I. Douair, L. Maron and M. Mazzanti, Accessing the +IV Oxidation State in Molecular Complexes of Praseodymium, *J. Am. Chem. Soc.*, 2020, **142**, 5538-5542.

16. K. Dehnicke, M. Krieger and W. Massa, Phosphoraneiminato Complexes of Transition Metals, *Coord. Chem. Rev.*, 1999, **182**, 19-65.

17. A. K. Maity, J. Murillo, A. J. Metta-Magaña, B. Pinter and S. Fortier, A Terminal Iron(IV) Nitride Supported by a Super Bulky Guanidinate Ligand and Examination of Its Electronic Structure and Reactivity, *J. Am. Chem. Soc.*, 2017, **139**, 15691-15700.

18. P. J. Bailey and S. Pace, The coordination chemistry of guanidines and guanidinates, *Coord. Chem. Rev.*, 2001, **214**, 91-141.

19. F. T. Edelmann, Lanthanide Amidinates and Guanidinates: From Laboratory Curiosities to Efficient Homogeneous Catalysts and Precursors for Rare-Earth Oxide Thin Films, *Chem. Soc. Rev.*, 2009, **38**, 2253-2268.

20. J. Francos and V. Cadierno, The Chemistry of Guanidinate Complexes of the Platinum group Metals, *Dalton Trans.*, 2019, **48**, 9021-9036.

21. C. Jones, Bulky Guanidinates for the Stabilization of Low Oxidation State Metallacycles, *Coord. Chem. Rev.*, 2010, **254**, 1273-1289.

22. M. P. Coles, Application of Neutral Amidines and Guanidines in Coordination Chemistry, *Dalton Trans.*, 2006, 985-1001.

23. D. Werner, G. B. Deacon, P. C. Junk and R. Anwander, Cerium(III/IV) Formamidinate Chemistry, and a Stable Cerium(IV) Diolate, *Chem. Eur.*, 2014, **20**, 4426-4438.

24. M. P. Coles, Bicyclic-Guanidines, -Guanidinates and -Guanidinium Salts: Wide Ranging Applications from a Simple Family of Molecules, *Chem. Commun.*, 2009, 3659-3676.

25. A. K. Maity, S. Fortier, L. Griego and A. J. Metta-Magaña, Synthesis of a "Super Bulky" Guanidinate Possessing an Expandable Coordination Pocket, *Inorg. Chem.*, 2014, **53**, 8155-8164.

26. M. Castillo, O. Barreda, A. K. Maity, B. Barraza, J. Lu, A. J. Metta-Magaña and S. Fortier, Advances in Guanidine Ligand Design: Synthesis of a Strongly Electron-Donating, Imidazolin-2-iminato Functionalized Guanidinate and its Properties on Iron, *J. Coord. Chem.*, 2016, **69**, 2003-2014.

27. P. Dröse, J. Gottfriedsen, Cristian G. Hrib, Peter G. Jones, L. Hilfert and Frank T. Edelmann, The First Cationic

Complex of Tetravalent Cerium, *Z. Anorg. Allg. Chem.*, 2011, **637**, 369-373.

28. J. A. Bogart, C. A. Lippincott, P. J. Carroll, C. H. Booth and E. J. Schelter, Controlled Redox Chemistry at Cerium within a Tripodal Nitroxide Ligand Framework, *Chem. Eur.*, 2015, **21**, 17850-17859.

29. Y.-M. So, Y. Li, K.-C. Au-Yeung, G.-C. Wang, K.-L. Wong, H. H. Y. Sung, P. L. Arnold, I. D. Williams, Z. Lin and W.-H. Leung, Probing the Reactivity of the Ce═O Multiple Bond in a Cerium(IV) Oxo Complex, *Inorg. Chem.*, 2016, **55**, 10003-10012.

30. L. A. Solola, P. J. Carroll and E. J. Schelter, Cationic Cerium(IV) Complexes with Multiple Open Coordination Sites, *J. Organomet. Chem.*, 2018, **857**, 5-9.

31. Y. Qiao, D.-C. Sergentu, H. Yin, A. V. Zabula, T. Cheisson, A. McSkimming, B. C. Manor, P. J. Carroll, J. M. Anna, J. Autschbach and E. J. Schelter, Understanding and Controlling the Emission Brightness and Color of Molecular Cerium Luminophores, *J. Am. Chem. Soc.*, 2018, **140**, 4588-4595.

32. R. D. Shannon, Revised Effective Ionic Radii and Systematic Studies of Interatomic Distances in Halides and Chalcogenides, *Acta Crystallogr. A*, 1976, **32**, 751-767.

33. N. Elgrishi, K. J. Rountree, B. D. McCarthy, E. S. Rountree, T. T. Eisenhart and J. L. Dempsey, A Practical Beginner's Guide to Cyclic Voltammetry, *J. Chem. Ed.*, 2018, **95**, 197-206.

34. M. K. Assefa, D.-C. Sergentu, L. A. Seaman, G. Wu, J. Autschbach and T. W. Hayton, Synthesis, Characterization, and Electrochemistry of the Homoleptic f Element Ketimide Complexes [Li]$_2$[M(N═C^{t}BuPh)$_6$] (M = Ce, Th), *Inorg. Chem.*, 2019, **58**, 12654-12661.

35. E. M. Broderick, P. S. Thuy-Boun, N. Guo, C. S. Vogel, J. Sutter, J. T. Miller, K. Meyer and P. L. Diaconescu, Synthesis and Characterization of Cerium and Yttrium Alkoxide Complexes Supported by Ferrocene-Based Chelating Ligands, *Inorg. Chem.*, 2011, **50**, 2870-2877.

36. J. A. Bogart, A. J. Lewis, S. A. Medling, N. A. Piro, P. J. Carroll, C. H. Booth and E. J. Schelter, Homoleptic Cerium(III) and Cerium(IV) Nitroxide Complexes: Significant Stabilization of the 4+ Oxidation State, *Inorg. Chem.*, 2013, **52**, 11600-11607.

37. H. Yin, P. J. Carroll, B. C. Manor, J. M. Anna and E. J. Schelter, Cerium Photosensitizers: Structure–Function Relationships and Applications in Photocatalytic Aryl Coupling Reactions, *J. Am. Chem. Soc.*, 2016, **138**, 5984-5993.

38. X. Qin, X. Liu, W. Huang, M. Bettinelli and X. Liu, Lanthanide-Activated Phosphors Based on 4f-5d Optical Transitions: Theoretical and Experimental Aspects, *Chem. Rev.*, 2017, **117**, 4488-4527.

39. H. Yin, P. J. Carroll, J. M. Anna and E. J. Schelter, Luminescent Ce(III) Complexes as Stoichiometric and Catalytic Photoreductants for Halogen Atom Abstraction Reactions, *J. Am. Chem. Soc.*, 2015, **137**, 9234-9237.

40. H. E. Hoefdraad, Charge-transfer Spectra of Tetravalent Lanthanide Ions in Oxides, *J. Inorg. Nucl. Chem.*, 1975, **37**, 1917-1921.

41. M. W. Löble, J. M. Keith, A. B. Altman, S. C. E. Stieber, E. R. Batista, K. S. Boland, S. D. Conradson, D. L. Clark, J. Lezama Pacheco, S. A. Kozimor, R. L. Martin, S. G. Minasian, A. C. Olson, B. L. Scott, D. K. Shuh, T. Tyliszczak,

M. P. Wilkerson and R. A. Zehnder, Covalency in Lanthanides. An X-ray Absorption Spectroscopy and Density Functional Theory Study of $LnCl_6^{x-}$ (x = 3, 2), *J. Am. Chem. Soc.*, 2015, **137**, 2506-2523.

42. R. L. Halbach, G. Nocton, J. I. Amaro-Estrada, L. Maron, C. H. Booth and R. A. Andersen, Understanding the Multiconfigurational Ground and Excited States in Lanthanide Tetrakis Bipyridine Complexes from Experimental and CASSCF Computational Studies, *Inorg. Chem.*, 2019, **58**, 12083-12098.

43. C. H. Booth, M. D. Walter, M. Daniel, W. W. Lukens and R. A. Andersen, Self-Contained Kondo Effect in Single Molecules, *Phys. Rev. Lett.*, 2005, **95**, 267202.

44. R. L. Halbach, G. Nocton, C. H. Booth, L. Maron and R. A. Andersen, Cerium Tetrakis(tropolonate) and Cerium Tetrakis(acetylacetonate) Are Not Diamagnetic but Temperature-Independent Paramagnets, *Inorg. Chem.*, 2018, **57**, 7290-7298.

45. D. E. Smiles, E. R. Batista, C. H. Booth, D. L. Clark, J. M. Keith, S. A. Kozimor, R. L. Martin, S. G. Minasian, D. K. Shuh, S. C. E. Stieber and T. Tyliszczak, The duality of electron localization and covalency in lanthanide and actinide metallocenes, *Chem. Sci.*, 2020, **11**, 2796-2809

46. M. D. Walter, C. H. Booth, W. W. Lukens and R. A. Andersen, Cerocene Revisited: The Electronic Structure of and Interconversion Between $Ce_2(C_8H_8)_3$ and $Ce(C_8H_8)_2$, *Organometallics*, 2009, **28**, 698-707.

47. S. G. Minasian, E. R. Batista, C. H. Booth, D. L. Clark, J. M. Keith, S. A. Kozimor, W. W. Lukens, R. L. Martin, D. K. Shuh, S. C. E. Stieber, T. Tylisczcak and X.-d. Wen, Quantitative Evidence for Lanthanide-Oxygen Orbital Mixing in CeO_2, PrO_2, and TbO_2, *J. Am. Chem. Soc.*, 2017, **139**, 18052-18064.

Journal Name

ARTICLE

TOC
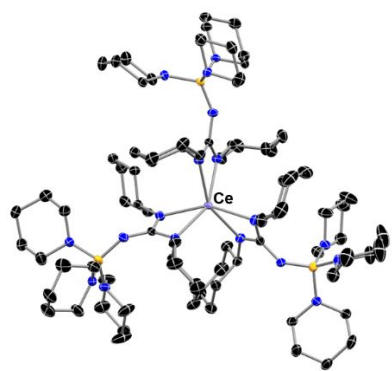
[Ce^{IV}(^{Cy}GNP(pip)$_3$)$_3$]BPh$_4$
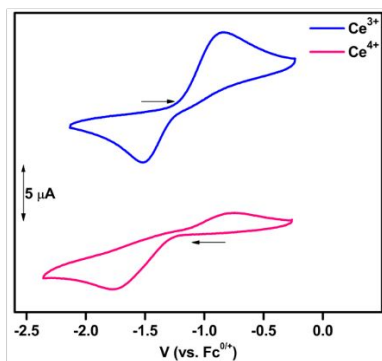
Ce^{4+}
E$_{pc}$ = -1.98 V, E$_{pa}$ = -0.47 V (800 mV/s, THF, vs Fc$^{0/+}$)

The synthesis of a *tris*(piperdino)imidophosphorane N,N'-dicyclohexylguanidinate ligand and its Ce^{3+} and Ce^{4+} tris-homoleptic compounds is reported.